



Solid-Liquid Extraction of Uranium from Nitrate Medium using Macroporous Cation Exchange Resin; Kinetics and Thermodynamics Studies

Ahmed A. Abdelsamad

Nuclear Materials Authority, Egypt

E-mail :ahmed_smd@hotmail.com

Abstract

Sorption characteristics of uranium onto the strongly acidic cation exchanger, Purolite C100, were investigated. Uranium sorption capabilities of the adsorbent were estimated by Batch experiments under different conditions; pH, contact time, uranium initial concentration, temperature, adsorbent dose, interfering ions, and agitation speed. The characteristics of Purolite C100 were determined using scanning electron microscopy (SEM) and FTIR spectra. Also, the sorption kinetics and equilibrium parameters were determined. At the optimum conditions, the adsorption capacity of uranium was found to be nearly 175 mg/g. The kinetics and isotherm studies could show that the uranium sorption onto Purolite C100 is following the pseudo-second-order model. Uranium sorption is fitted with Langmuir isotherm. Thermodynamic studies indicated an exothermic behavior with an increase in randomness. The studied procedure was used for uranium ions removal from the raffinate solution obtained from the solvent extraction unit, Nuclear Materials Authority, Egypt.

Keywords: Uranium, Nitrate media, Purolite C100, Kinetics, Isotherm models, Thermodynamics, Raffinate solution

Received; 15 Sept. 2020, Revised form; 21 Dec. 2020, Accepted; 21 Dec. 2020, Available online 1 Jan. 2021

1. Introduction

Substantial research efforts were orientated to the development of efficient and economically feasible methods for the recovery of uranium. These methods include ion exchange, co-precipitation, solvent extraction, membrane-based separation, and adsorption on various surfaces [1-5].

Solid-liquid extraction of uranium from its resources has proved to be more advantageous because of the total insolubility of the applied solid in the aqueous phase, its low rate of physical degradation besides its high sorption

capacity as well as its good flexibility and kinetic properties [6,7]. In this respect, ion-exchange methods are widely used for the hydrometallurgical recovery of uranium from acidic leached mineral ore bodies [8].

Many types of ion exchange resins have been tried for the separation of uranium [9-14].

Gawad [15] studied the adsorption behavior of uranium ions from nitrate solutions using the strong acid cation exchange Amberlite IR120 resin. The adsorption parameters have been optimized. The physical parameters including the adsorption kinetics, the isotherm models, and the thermodynamic data have been determined to describe the nature of the uranium adsorption by the investigated resin. The modeled data has been found to agree with both the exothermic pseudo-first-order reaction and the Langmuir isotherm.

Taha [16] used a series of Purolite commercial resins: sulfonic cationic exchanger (MTC1600H), amino phosphonic-chelating resin (MTS9500), and phosphonic/sulfonic chelating resins (MTS9570) for uranium adsorption from crude dihydrate phosphoric acid. The impact of various parameters on the sorption efficiency

such as shaking time, sorbent dose, phosphoric acid concentration, and reaction temperature has been investigated. The obtained data showed that the chelating resins MTS9500 and MTS9570 exhibit higher sorption efficiency than the cationic exchange resin MTC1600H. Kinetic, isotherms, and thermodynamics analysis for the obtained data has been performed.

Anirudhan and Radhakrishnan [17] prepared a new cation exchange resin (PGTFS-COOH) having a carboxylate functional group at the chain end by grafting poly(hydroxyethyl methacrylate) onto tamarind fruit shell, TFS (a lignocellulosic residue) using potassium peroxydisulphate-sodium thiosulphate redox initiator, and in the presence of N, N'-methylene bisacrylamide (MBA) as a crosslinking agent. The kinetic and sorption isotherm data fitted with the pseudo-second-order equation and Sips isotherm model. An increase in temperature induced a positive effect on the adsorption process. The calculated activation energy of adsorption indicated that U(VI) adsorption was largely due to the diffusion-controlled process. The values of adsorption enthalpy, Gibbs free energy, and entropy were calculated using thermodynamic function relationships.

Abdelal and Abdelsamad [18] studied different parameters affecting the extraction of uranium from its solution using the anion exchange resin, Amberlite IRA400, by using both the Batch method and fixed column techniques.

The sorption characteristics of uranium onto a strongly basic anion exchanger, Purolite A400, were investigated by Masoud [19]. The adsorption capacity of uranium was found to be nearly 117.6 mg/g. The kinetics and isotherm

studies could show that the uranium sorption onto Purolite A400 is following the models of pseudo-second-order and Langmuir isotherm. The thermodynamic parameters had indicated that the adsorption of uranium is an exothermic and spontaneous process.

Ahmad [20] prepared Quinoline Silicate Lewatit Composite (QSLC) and activated Lewatit (AL), they were tested for uranium removal from sulfate solution. Experimental data obeyed the Langmuir isotherm model with 69.44 mg/g and 217.39 mg/g theoretical capacity for AL and QSLC, respectively. Thermodynamic studies indicated an exothermic behavior with a decrease in randomness. Kinetics studies showed that the adsorption process obeyed the pseudo-second-order model. Optimum conditions were carried out for uranium recovery from a rock sample, producing uranium concentrate with 93.33% purity.

Purolite C100 has been used successfully for water treatment purposes [21, 22]. So far no published work is reported for the use of this resin for uranium uptakes.

The present work is mainly concerned with the application of commercial grade of Purolite C100 which is available in the domestic market, in nuclear activities. The objective of this work is also to focus on establishing the parameters that may affect the rate of uranium extraction from aqueous solution, as a function of the adsorbent. Furthermore, optimization of the most proper operating conditions of uranium removal onto the introduced adsorbent will take place during this study. The obtained

Table (1): The physical and chemical characteristics of strongly base Purolite C100 resin.

<u>Polymer Structure</u>	<u>Gel polystyrene crosslinked with divinylbenzene</u>
<u>Appearance</u>	<u>Spherical Beads</u>
<u>Functional Group</u>	<u>Sulfonic Acid</u>
<u>Total Capacity</u>	<u>2.0 eq/L (43.7 Kgr/ft³) (Na⁺ form)</u>
<u>Moisture Retention</u>	<u>44 - 48 % (Na⁺ form)</u>
<u>Ionic Form</u>	<u>Na⁺ form</u>
<u>Particle Size Range</u>	<u>300 - 1200 μm</u>
<u>< 300 μm (max.)</u>	<u>1 %</u>
<u>Uniformity Coefficient (max.)</u>	<u>1.7</u>
<u>Reversible Swelling,</u>	
<u>Na⁺ → H⁺ (max.)</u>	<u>8 %</u>
<u>Specific Gravity</u>	<u>1.29</u>
<u>Shipping Weight (approx.)</u>	<u>800 - 840 g/L (50.0 - 52.5 lb/ft³)</u>
<u>Temperature Limit</u>	<u>120 °C (248.0 °F)</u>

N-phenyl anthranilic acid as well as Arsenazo III were obtained from Merck. Uranyl nitrate was supplied from Riedel–deHaen. Ammonium vanadate, bromine, Urea, KBr, and FeSO₄·7H₂O were obtained from Scharlau Chemie. Nitric acid and sodium hydroxide were obtained from Sigma-Aldrich. Double distilled water was used for the preparation of aqueous solutions.

2.3. Preparation of synthetic uranyl nitrate solution

The uranyl nitrate synthetic solutions were prepared by dissolving the exact amount of uranyl nitrate in a suitable amount of acidified distilled water.

2.4. Adsorption and stripping procedures

Batch adsorption experiments were performed by stirring a known volume and concentration of uranium solution

results were applied to the separation of uranium from the raffinate solutions as real samples in terms of waste management obtained from the solvent extraction unit, Nuclear Materials Authority, Egypt.

2. Experimental

2.1. Instrumentation

Complete characterization of Purolite C100 was carried out using Fourier transform infrared spectrometer (FT-IR, Thermo Scientific, NICOLET IS10, USA) to determine the major functional groups of the presented resin. The surface morphology of Purolite C100 was studied by scanning electron microscope model JEOL-JSM-5600LV.

Uranium was analyzed in the aqueous solution by oxidimetric titration vs. ammonium metavanadate [23]. Results were confirmed by UV-vis spectrophotometer at a wavelength of 655 nm (SP-8001 UV-, Metretech Inc. version 1.02, 2000/10/01) that contains a glass cell of 10 mm was used for determining uranium concentration using Arsenazo III as a reagent [24].

ICP (Prodigy Axial high dispersion ICP-OES-USA) and atomic absorption model (G.B.C.A.A) were used for determining the constituent and trace elements in the raffinate solutions.

2.2. Chemicals and reagents

Purolite resin (Purolite C100) was conducted from Purolite Co Ltd, Qianyuan-China. Table (1) summarizes the main properties of the resin. All chemicals and reagents used are of analytical grade.

with a certain amount of adsorbent at controlled time and temperature till equilibrium is achieved. The effect of different controlling factors, e.g. pH, contact time, initial uranium concentration, temperature, adsorbent dose, interfering ions, and agitation speed were studied. At each experiment, uranium was measured in the filtrate. The adsorption efficiency (E %) was calculated from the following relation:

$$E\% = \frac{C_o - C_e}{C_o} \times 100 \quad (1)$$

where C_o is initial uranium concentration, C_e equilibrium uranium concentration.

The uranium uptake capacity q_e (mg/g) is calculated by the relation:

$$q_e = (C_o - C_e) \times \frac{V}{m} \quad (2)$$

Where; V is the volume of the aqueous solution and m is the mass of the dry resin. The distribution coefficient (K_d) is calculated from the following equation:

$$K_d = \frac{C_o - C_e}{C_e} \times \frac{V}{m} \quad (3)$$

Nitric acid, 1.0 M, is used as a stripping agent to recover uranium from the loaded adsorbent. 0.05 g of loaded adsorbent was shaken with 25 mL of a stripping agent for 30 min. at 25 °C. The concentration of the metal ion was determined in the aqueous phase after stripping to determine the stripping percent for the studied metal by equation (4).

$$\text{U Stripping Efficiency, \%} = \frac{C_e}{C_i} \times 100 \quad (4)$$

Where C_i is uranium conc. on the loaded resin and C_e is uranium conc. in stripping solution.

3. Results and discussion

3.1. Factors affecting uranium adsorption

3.1.1. Effect of pH

The pH of the aqueous solution can influence the aqueous chemistry of uranium [25]. The mobility of present ions in the medium is affected by the concentration of H^+ ions. Moreover, it also affects the capacity of adsorbents for target species. The effect of initial solution pH was investigated by preparing a series solution having a different pH within the range 1 to 6. 0.04 g of each adsorbent was allowed to contact with 10 mL of an aqueous solution of U (VI) of conc. 228 mg/L at 25 °C for 150 minutes at 100 rpm as agitation speed. Results shown in Figure (1), clarifies that uranium adsorption increases from pH 1 to 2.6. Beyond pH 3.0, the adsorption efficiency decreases with pH elevation. The optimum pH for adsorption is 2.6

monovalent $UO_2NO_3^+$ and Bivalent UO_2^{2+} cationic species were found to be dominant at lower pH using Hydra-Medusa software as shown in Figure (2).

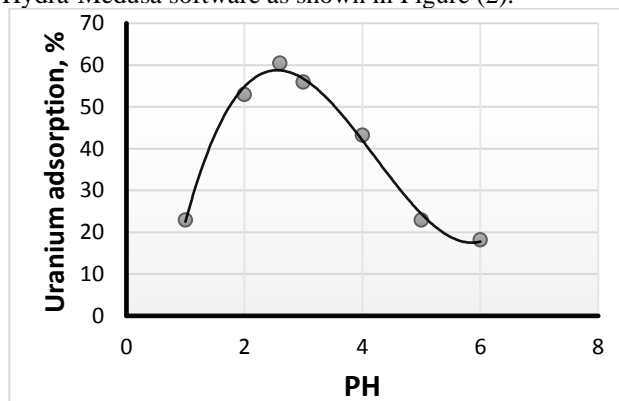


Fig (1): Effect of the pH of solution on uranium adsorption efficiency.

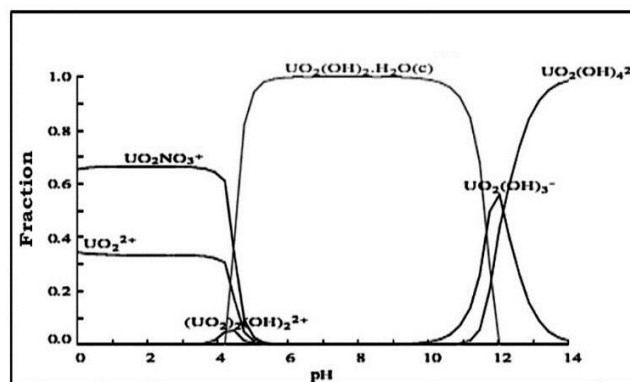


Fig (2): Uranium species calculated by hydra/Medusa, uranium conc. = 228 mg/L, T=25C° in 1 M HNO₃.

3.1.2. Effect of Contact Time

To determine the effect of contact time upon uranium adsorption efficiency, many experiments were studied to reach equilibrium in the range of 15 to 150 minutes. The other identical extraction conditions were fixed with 10 mL 228 mg/L uranium concentration at pH 2.6 and using 0.04 g from the resin at room temperature and 100 rpm. The results were plotted in Figure (3), this shows that the adsorption efficiency gradually increases with increasing the contact time. The sorption equilibrium has been reached after 120 min. where uranium sorption efficiency was 60.5 %. Further increase in reaction time has a slight impact on sorption efficiency. Hence, the adsorption equilibrium time considered for further work was taken as 120 min. for economic aspects.

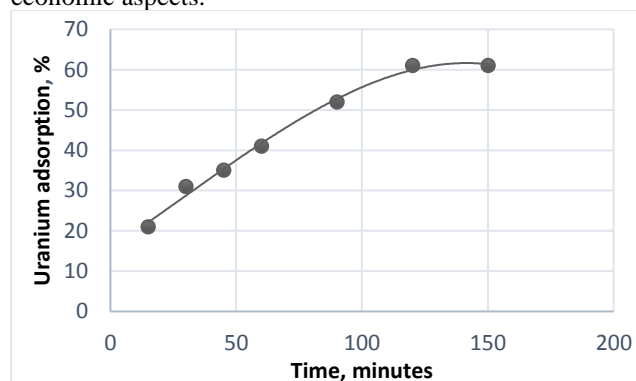


Fig (3): Effect of contact time on uranium adsorption efficiency.

3.1.3. Effect of initial uranium concentration

A series of 10 mL of uranium solution content varying from (100–4200 mg/L) was prepared to study the effect of initial uranium concentration on adsorption efficiency. In each experiment, the prepared solution was contacted for 120 minutes with 0.04 g of adsorbent at 100 rpm. The pH was retained at 2.6 for best results. Figure (4) illustrates the effect of initial uranium content in terms of adsorption efficiency and maximum uranium uptake (q_e). The adsorption efficiency ranged from 96.9 to 60.5% along with 100–228 mg/L uranium content and gradually declined to 16.6 % at initial uranium content of 4200 mg/L. The increase in uranium ions concentration leads to competition on the available active sites on the adsorbent surface, causing a dramatic decrease in adsorption efficiency [26].

Therefore, it can be ascertained that the maximum loading capacity of uranium on the purolite C100 is 175 mg/g.

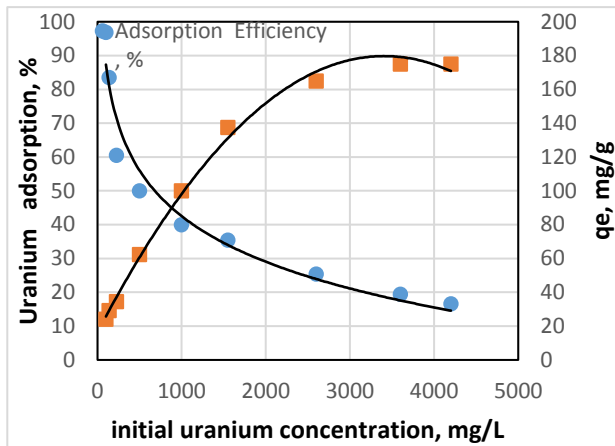


Fig (4): Effect of initial uranium concentration on uranium adsorption efficiency.

3.1.4. Effect of temperature

The effect of temperature on uranium adsorption was studied using 0.04 g of purolite C100 contacted with 10 mL of uranium solution of conc. 228 mg/L at pH 2.6 for 120 minutes at 100 rpm and different temperatures. Results shown in Figure (5) illustrate that uranium adsorption decreased linearly from 60.5 to 35 % with increasing temperature from 25 to 65 °C. Such behavior is due to the exothermic nature of the uranium adsorption process. The most suitable temperature that corresponds to the most efficient uranium adsorption was considered as the room temperature.

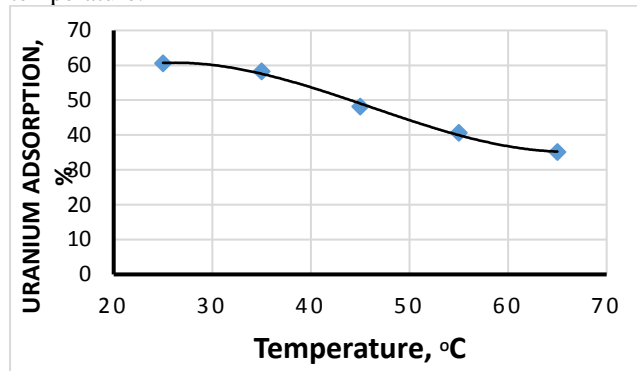


Fig (5): Effect of temperature on uranium adsorption efficiency.

3.1.5. Effect of resin amount

A series of adsorption experiments were performed using different adsorbent doses ranging from 0.01 up to 0.08 g resin contacted with 10 mL of uranium solution of conc. 228 mg/L at pH 2.6 for 120 minutes at room temperature and 100 rpm. The influence of the adsorbent amount on the adsorption of uranium was represented in Figure (6). The results revealed that the adsorption efficiency increases from 23.5 to 74 % with increasing adsorbent amount from 0.01 to 0.06g resin/10 ml. Further increase of the Purolite C100 resin amount the active sites become more plentiful than the available uranium ions in the solution. Consequently, the adsorptive capacity of the adsorbent available was not fully utilized at a higher adsorbent

amount. Based on the latter, 0.06 g Purolite C100 resin/10 mL is preferred as the usable adsorbent amount.

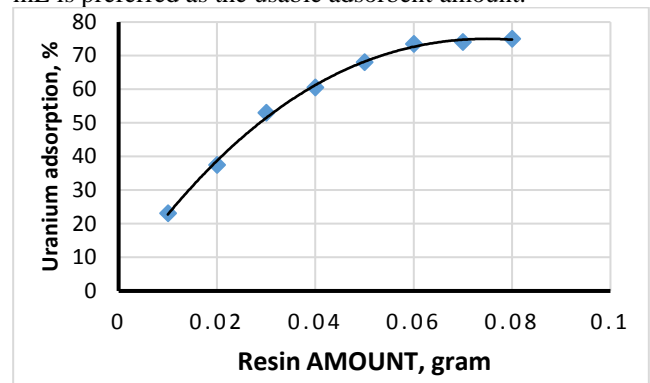


Fig (6): Effect of resin amount on uranium adsorption efficiency.

3.1.6. Effect of interfering ions

The effect of different interfering ions concentration on uranium adsorption efficiency using Purolite C100 was investigated. Na⁺, K⁺, Ca²⁺, Mg²⁺, Al³⁺, Fe³⁺, and Mn²⁺ were chosen as interfering elements because they are present in the matrix of the studied raffinate solution, as a case study. Different concentrations of stock solution of these cations were prepared. Results in Table (2), showed that the presence of all cations might slightly interfere with the uranium adsorption process except iron. Presence of iron suggesting competition with uranium ions and binding sites of Purolite C100.

Table (2): Effect of interfering ions on uranium adsorption by purolite C100

Elements	Conc.	50	75	100
	Uranium adsorption %			
Mn		73.9	71.5	70.5
Fe		70.2	63	60.9
Mg		74	73.8	70.8
Ca		73.8	73.7	73.5
Na		73.9	72.9	71.6
Al		73.8	73.4	71.2
K		72.1	71.1	71.1

3.1.7. Effect of Agitation Speed

The effect of the agitation speed was studied in the range between 50–300 rpm and 10 mL uranium solution of conc. 228 mg/L contacted for 120 minutes at room temperature contacted with pH 2.6. The adsorption percent of uranium increased to 88% as the stirring rate increased to 200 rpm then remained constant by increasing agitation speed. Therefore, the preferred speed was 200 rpm. The results are shown in Figure (7).

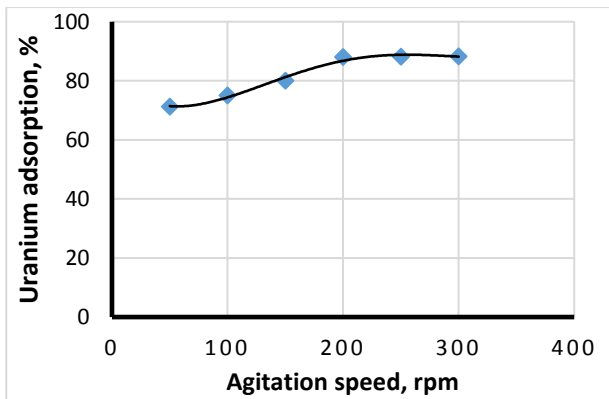


Fig (7): Effect of Agitation speed on the adsorption of uranium onto purolite C100.

3.2. Sorption kinetics and mechanism

Kinetic studies reveal information about the adsorption mechanism as well as the adsorption rate. In this respect, the experimental results of uranium adsorption using Purolite C 100 sorbents at solution pH of 2.6, resin amount 0.06 g/10ml, and at 25 ± 1 °C were as evaluated by using the simple Lagergren equation (5) and second-order kinetic equation (6) to determine the rate of the adsorption interactions [27-29].

$$\text{Log}(q_e - q_t) = \text{Log}q_e - \left(\frac{K_1}{2.303} \right) t$$

(5)

$$\frac{t}{q_t} = \frac{1}{K_2 q_e^2} + \left(\frac{1}{q_e} \right) t$$

(6)

where q_e and q_t are the amount of uranium adsorbed per unit mass of Purolite C100 (mg g^{-1}) at equilibrium and at time t , respectively. K_1 and K_2 are the pseudo-first-order rate constant (min^{-1}), and the second-order rate constant ($\text{g. mg}^{-1}. \text{min}^{-1}$), respectively. K_1 values were obtained by plotting $\log(q_e - q_t)$ versus t for adsorption of uranium (Figure (8)), while K_2 values were obtained from the kinetic plot of t/q_t versus t for uranium adsorption (Figure (9)).

As seen from Figure (8), the adsorption of uranium by Purolite C100 is not fitted well with the pseudo-first-order model due to the lack of linearity ($R^2 = 0.93$), and the calculated maximum adsorption capacity is far away from that obtained experimentally, Table (3). On the other hand, Figure (9) showed a straight line with correlation coefficients closer to unity. Moreover, the calculated equilibrium adsorption capacity (q_e) is consistent with the experimental data. Therefore, the adsorption reaction is likely explained by the pseudo-second-order adsorption. The values of the second-order rate constant (K_2) and correlation coefficient (R^2) were listed in Table (3).

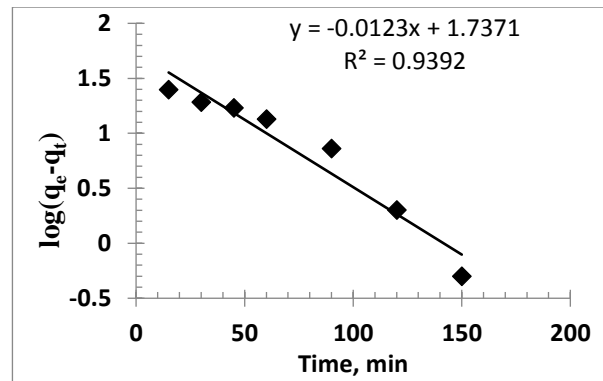


Fig (8): Pseudo-first-order plot for the adsorption of uranium on Purolite C100.

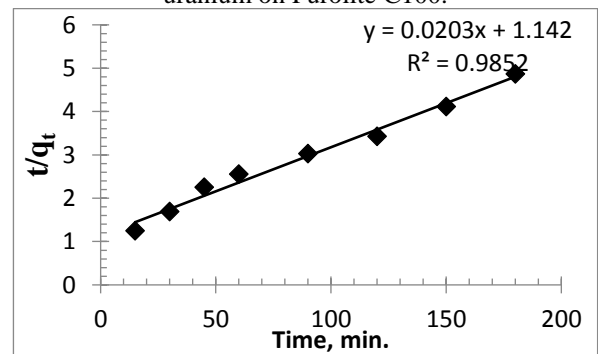


Fig (9): Pseudo-second order kinetics for the adsorption of uranium on Purolite C100.

Table (3): The calculated parameters of the pseudo-first-order and pseudo-second-order models.

Lagergren pseudo first-order	K_1 (min^{-1})	0.028
	$q_{e, \text{cal}}$ (mg/g)	37
	$q_{e, \text{exp}}$ (mg/g)	54.5
	R^2	0.93
Pseudo-second-order	K_2 (min^{-1})	0.87
	$q_{e, \text{cal}}$ (mg/g)	37
	$q_{e, \text{exp}}$ (mg/g)	46.2
	R^2	0.98

The study which links two factors simultaneously to achieve workable accuracy results is to be considered as an important step within a great achievement. So Software such as MATLAB program can simulate this link graphically after constructing proper m-files. Herein, "cftool", "ezyfit", and some functions which are suitable for achieving this target [30].

Non-linear forms nowadays are the effect choice not only for accuracy demands but further dealing to enlarge the models beneficitation as well. Emphasis on the accuracy when simulating the model -itself and its chain rings- gives a good realizing the system criteria. This is in general can aid many workers who look forward to a quick effect modeling and simulation as a front end of many advanced processes or for saving a lot of effort, time, and financial burdens.

By using MATLAB program, by plot time against uranium concentration remained we note that reaction takes

place in two parallel steps each step is a pseudo-first-order reaction, and the reaction can be expressed by the following equation:

$$U \text{ conc.} = a \times e^{-k_1 t} + c \times e^{-k_2 t} \quad (7)$$

Data from figure (10) show that correlation coefficient equal 0.993, $a = 41.91 \text{ ppm}$, $k_1 = 0.1047$, $c = \text{initial concentration} - a = 186.1 \text{ ppm}$, and $k_2 = 0.0056$.

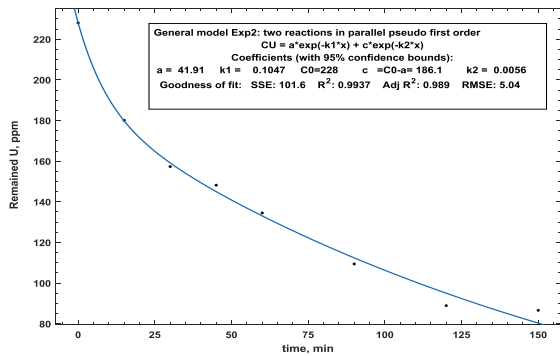


Fig (10): Determination of the n order of reaction (two parallel pseudo-first-order reactions).

The data are fitted with pseudo n^{th} order rate equation which can be derived as follow for any pseudo n order [30]:

$$\frac{dq}{dt} = k (q_e - q_t)^n \quad (8)$$

Which on separation and integration yields

$$q_t = q_e - \left(q_e^{(1-n)} + (k (n - 1) t) \right)^{1/(1-n)} \quad (9)$$

Figure (11) simulates eq. (9) and declares that in a workable approximation the pseudo-second-order is the predominant kinetic model.

The calculated equilibrium adsorption capacity (q_e) is consistent with the experimental data. The obtained data featured in Fig. (11) show that the process can be approximated more satisfactorily by the pseudo-second-order as the predominant mechanism.

The general model of pseudo n order reaction was applied to get the order of total reaction by MATLAB via plot time against q_e Fig.(11) by using the following equations [30]:

$$q_t = q_e - (q_e^{(1-n)} + (k \times (n-1) t))^{1/(1-n)} \quad (10)$$

$$q_t = q_e - (q_e^{(1-n)} + (k \times (n-1) t))^{1/(1-n)} \quad (11)$$

$$q_{(t,T)} = q_e - (q_e^{(1-n)} + ((n-1) \times t \times A_r \times \exp(-\Delta E \times 1000 / (8.314 \times T)))^{1/(1-n)} \quad (12)$$

Where A_r , ΔE , and K are Arrhenius frequency factor, activation energy, and rate of reaction respectively.

We found that correlation coefficient equal 0.986, $k = 0.000805$, $n = 1.608$, $q_e = 175 \text{ mg/g}$. n value indicates the total reaction is belongs to second order reaction and q_e value confirmed the value of maximum capacity obtained

from experimental data.

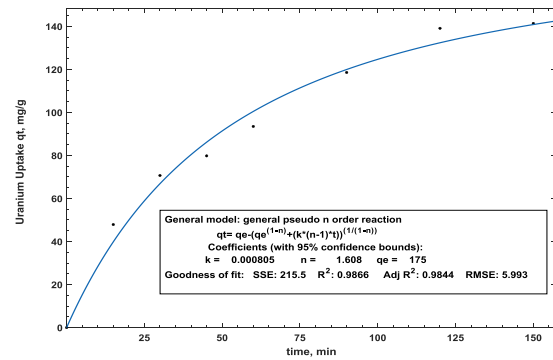


Fig (11): Determination of the Kinetic Model of total reaction (general pseudo n order reaction).

3.3. Adsorption isotherm models

The adsorption isotherm provides the most important information about how the adsorbed molecules are distributed between the solid and aqueous phases when the adsorption process reaches an equilibrium state. For this purpose, the uranium adsorption on Purolite C100 has been described by applying the most widely used Langmuir and Freundlich isotherm models [31, 32]. The Langmuir isotherm considers the adsorption as a chemical phenomenon with the formation of an energetical monolayer with a maximum adsorption capacity of q_{max} (mg/g) through the following Equation (13):

$$\frac{C_e}{q_e} = \frac{C_e}{q_{\text{max}}} + \frac{1}{K_L q_{\text{max}}} \quad (13)$$

where K_L is a constant of the adsorption equilibrium (L/mg), q_{max} is the saturated monolayer adsorption capacity (mg/g), while q_e and C_e are the uranium uptake capacity (mg/g) of adsorbent and the residual uranium concentration (mg/L) at equilibrium. A linearized plot of C_e/q_e against C_e gives q_{max} and K_L as shown in Figure (12).

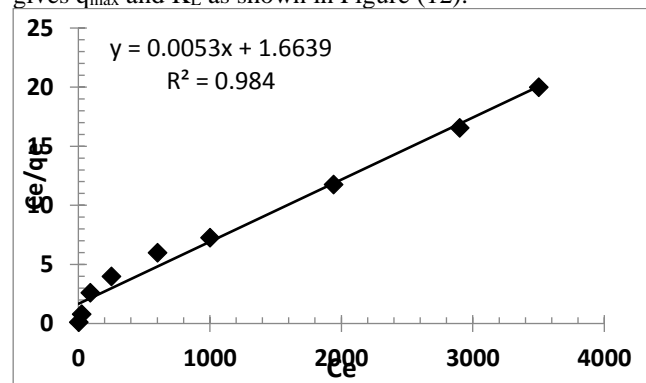


Fig (12): Langmuir adsorption isotherm model of U (VI) on Purolite C100.

Freundlich Equation (14) which, based on adsorption on heterogeneous surface could be expressed as the following:

$$\text{Log} q_e = \text{Log} K_f + \frac{1}{n} \text{Log} C_e \quad (14)$$

K_f and n are the Freundlich constants which represent the adsorption capacity and the adsorption intensity respectively. K_f and n can be determined from a linear plot of $\text{Log} q_e$ against $\text{Log} C_e$ as shown in Figure (13). The

results of the Langmuir and Freundlich isotherm constants are given in Table (4). It is found that uranium adsorption on pourlite C100 correlates quite well ($R^2 > 0.98$) with the Langmuir equation as compared with the Freundlich equation under the studied concentration range. Langmuir model is thus suitable for the description of the adsorption equilibrium of uranium onto pourlite C100. The essential characteristics of the Langmuir isotherm can be expressed in terms of a dimensionless constant separation factor [33], R_L , which is used to predict if an adsorption system is favorable or not. The separation factor, R_L , is given by the following Eq. (15):

$$R_L = \frac{1}{1 + K_L C_0} \quad (15)$$

where C_0 is the initial uranium (VI) concentration (mg/L) and K_L is the Langmuir adsorption constant (L/mg). The calculated R_L value for uranium (VI) concentration of 228 mg U/L is 0.123 which was in the range of 0.0 to 1.0 and indicates that the adsorption of uranium (VI) on Puroilite C100 is favorable.

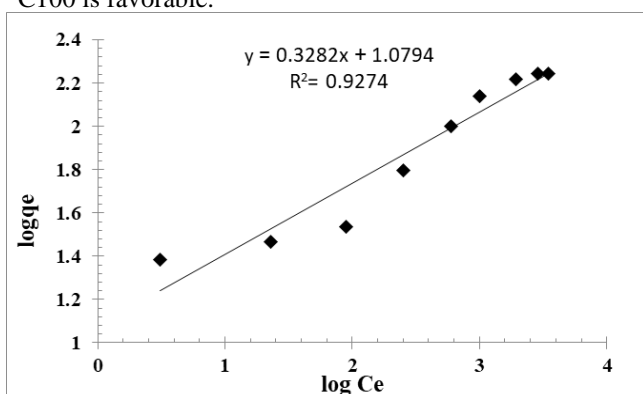


Fig (13): Freundlich adsorption isotherm model of U (VI) on Puroilite C100.

Table (4): Isotherm model constants.

Freundlich isotherm model	K_f (mg/ g)	12
	n	3.04
	R^2	0.92
Langmuir isotherm model	Q_m (mg/g)	188
	K_L	0.031
	R^2	0.98

Langmuir, Freundlich, and [Brunauer– Emmett– Teller (BET) and Redlich–Peterson as derivatives function from Langmuir] isotherms models were applied by MATLAB as common adsorption isotherm models to fit the attained isotherm data under the equilibrium adsorption of the Puroilite C100 resin.

-Langmuir model: equation (13) can be written as,

$$q_e = q_{max} \frac{kC_e}{(1 + kC_e)} \quad (16)$$

A non-linear simulation of equation (14) produced the corresponding parameters are presented in Fig. (14) and Table (5). The values of q_{max} (205.3 mg/g) and k 0.001878 L/mg, with R^2 equal to 0.9667. It means that Langmuir is anticipated as the represented isotherm for this system.

-The Freundlich model: The empirical model was shown to be consistent with the exponential distribution of active centers, characteristic of heterogeneous surfaces [34]. Equation (14) can be written as:

$$q_e = K_f C_e^{1/n} \quad (17)$$

Freundlich constants of this work are given in Table (5), $R^2 = 0.96$ which reveals that Freundlich isotherm model can't represent this system.

-Redlich–Peterson isotherm [35] is a hybrid isotherm Table (5): Langmuir, BET, Redlich–Peterson and Freundlich parameters for uranium adsorption on to pourlite C100 resin featuring both Langmuir and Freundlich isotherms, which incorporate three parameters into an empirical equation. The model has a linear dependence on concentration in the numerator and an exponential function in the denominator to represent adsorption equilibria over a wide concentration range, that can be applied either. Typically, a minimization procedure is adopted in solving the equations by maximizing the correlation coefficient between the experimental data points and theoretical model predictions. Redlich–Peterson isotherm is given by the following equation (18):

$$q_e = \frac{k_R C_e}{(1 + a_R C_e^g)} \quad (18)$$

or as Langmuir family form,

$$q_e = q_m \frac{kC_e}{(1 + kC_e^n)} \quad (19)$$

Where k_R , a_R , and g are the Redlich–Peterson which represents saturated sorption capacity and the sorption equilibrium constant and sorption intensity respectively.

A non-linear simulation of equations (18 and 19) produced the corresponding parameters as seen in Fig (14). Redlich–Peterson constants are given in Table (5) which means that this isotherm is a mathematical function; (170.7 mg/g) and almost represents the practical uptake value 175 mg/g as shown previously.

-Brunauer–Emmett–Teller (BET) [36] isotherm is a theoretical equation, most widely applied in the gas-solid equilibrium systems. It was developed to derive multilayer adsorption systems with relative pressure ranges from 0.05 to 0.30 corresponding to a monolayer coverage lying between 0.50 and 1.50. Its extinction model related to the liquid-solid interface is exhibited as the following equation (20):

$$q_e = \frac{q_s C_{BET} C_e}{(C_s - C_e)[1 + (C_{BET} - 1)(C_e / C_s)]} \quad (20)$$

where C_{BET} , C_s , q_s , and q_e are the BET adsorption isotherm (L/mg), adsorbate monolayer saturation concentration (mg/L), theoretical isotherm saturation capacity (mg/g), and equilibrium adsorption capacity (mg/g), respectively. Practically q_s and (C_{BET} / C_s) are an analogy to q_{max} and k in the Langmuir model. BET constants are given in Table (5) which means that as mentioned in Redlich–Peterson isotherm this isotherm is a mathematical function; (205.3 mg/g). It almost represents the real uptake value of U, 175 mg/g. From Table (5): Although there is stiff competition among the four

isotherms, but Langmuir constants are more matching with the practical values. Therefore, Langmuir is satisfied to represent this system. The q_{max} provided by the producer is ~205 mg/g while the calculated q_{max} for the three isotherms is ~175 it means intermediate affinity to uranium.

although BET is overlapped Langmuir, Langmuir is the most suitable model because it has a higher correlation coefficient and passes through most points and it is Compatible with the previous results, and q_e value confirmed the value of maximum capacity obtained from experimental data.

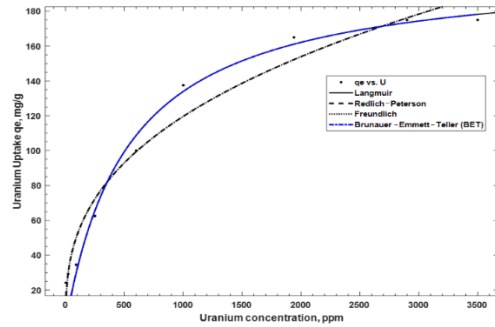


Fig (14): Isotherms plot for adsorption of uranium onto Poulite C100 using MATLAB

Table (5): Langmuir, BET, Redlich–Petersonand, and Freundlich parameters for uranium adsorption on Poulite C100 Rresin.

Isotherm	Parameters	Goodness Of fit			
		SSE*	R ²	adj R ²	RMSE**
Langmuir	k = 0.001878 qm = 205.3	1111	0.9667	0.9619	12.6
		1111	0.9667	0.9555	13.61
BET	C _{BET} = 4.9e+06 C _s =2.609e+09 mg/g C _{BET} /C _s = 0.0018 q _s = 205.3 mg/g				
Redlich-Peterson	k= 0.002292 n = 0.9807 qm = 170	1103	0.9669	0.9559	13.56
Freundlich	Kf = 9.743 n = 2.754	1094	0.9672	0.9625	12.5

*SSE: Sum of Squares Due to Error

** RMSE: Root Mean Squared Error

For both SSE and RMSE: A value closer to 0 indicates that the model has a smaller random error component and that the fit will be more useful for prediction

3.4. Thermodynamic Characteristics

The thermodynamics properties of the sorption process have been investigated to obtain the thermodynamic parameters: Gibb's free energy (ΔG°), enthalpy change (ΔH°), and entropy change (ΔS°). The following equations have been applied to calculate the thermodynamic parameters[37]:

$$\log K_d = \frac{\Delta H^\circ}{2.303RT} + A \quad (21)$$

$$\Delta G^\circ = 2.303RT \cdot \log K_d \quad (22)$$

$$\Delta G^\circ = \Delta H^\circ - T\Delta S^\circ \quad (23)$$

Where K_d is a nondimensional equilibrium constant, A is a constant, R is the universal gas constant (8.314 J/mol K), T is the temperature (K), ΔH° is the enthalpy change, ΔG° is the Gibbs free energy and ΔS° is the change in entropy. In this regard, the obtained data from the impact of temperature, ranging from 298 to 338 K, on uranium sorption onto Purolite C100 has been performed to determine the thermodynamic parameters for the sorption process as presented in Figure (15) and Table (6). Figure (15)

displayed a linear relationship between $\log K_d$ and $1/T$ (Van't Hoff equation) with correlation coefficient equals 0.96. The obtained data from Table 7 clarify that ΔH° has a negative value of about 12.11 kJ/mol, this means that the uranium sorption is an exothermic process. Within the temperature ranging from 293 to 328 K, the ΔG° values were found to be negative. This indicates that the uranium sorption process is spontaneous and favorable at the room temperature. The positive values of the ΔS° displayed the increase of the system randomness at the solid-liquid interface during the sorption process.

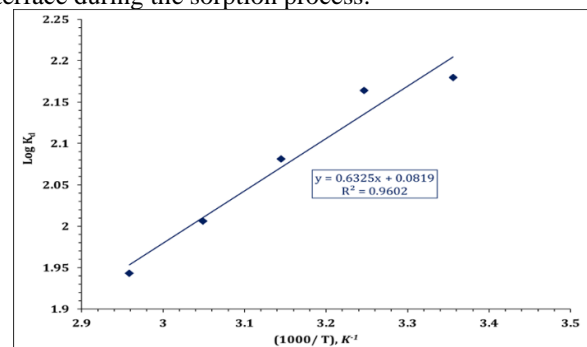


Fig (15): $\log K_d$ versus $1000/T$ for uranium sorption onto the Purolite C100.

Table (6): Thermodynamic data for sorption of uranium ions onto the PuroliteC100.

ΔG (kJ/mol)					ΔH kJ/mol	ΔS kJ/mol K ⁻¹
25°C	35°C	45°C	55°C	65°C	-12.11	1.11
-12.43	-12.76	-12.67	-12.59	-12.35		

3.5. Characterization of the resin (Purolite C100)

3.5.1. Scanning electron microscope (SEM)

(SEM) images of Purolite C100 before and after sorption of uranium from synthetic uranyl nitrate solution are shown in Figure 16. As can be seen in Figure 16(I), Purolite C100 particles are spherical with a uniformly planar surface. However, the surface became rough and wrinkled after the adsorption experiment, (Figure 16(II)). The change in surface topography can be attributed to the release of ions from the solution which was subsequently adsorbed on the resin surface.

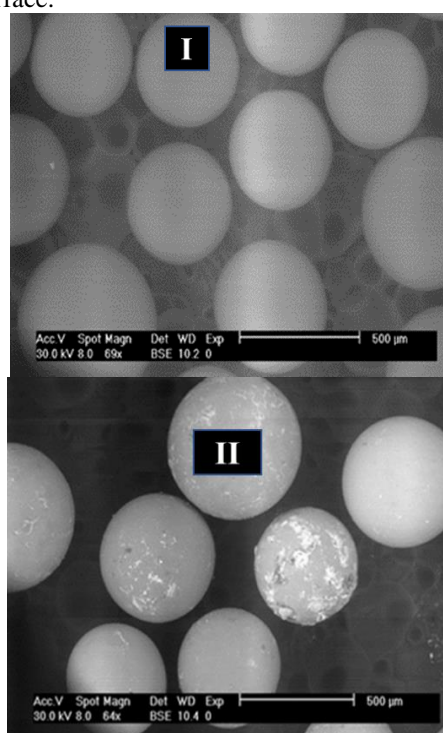


Fig (16): SEM micrographs of the adsorbent: (I) before uranium adsorption; and (II) after uranium adsorption.

3.5.2. Fourier transform infrared spectrometer characterization

The FTIR spectra of Purolite C100 before and after adsorption of uranium are given in Figure (17). The bands at 1540, 1513, 1455, and 1420 cm⁻¹ are attributed to aromatic C = C ring stretching. The peak at 756 cm⁻¹ is related to aromatic CH out of plane. Bands of 1122, 1060,

and 1051 cm⁻¹ indicate S–O vibration. 701 and 670 cm⁻¹ bands refer to the presence of C–S. The bands at about 2924 and 2922 cm⁻¹ were related to the stretching vibrations of the ring C–H bands of the resin (cross-linked polystyrene).

A signal corresponding to the vibration of O=U=O at 1122 cm⁻¹ was also observed, suggesting the uptake of U(VI) by studied resin [38, 39]. The intensity of some bands changed, and the transmittance of peaks was relatively greater in the case of loaded resin with U(VI) most bands were shifted, which also provided evidence of the interaction between U(VI) and the resin.

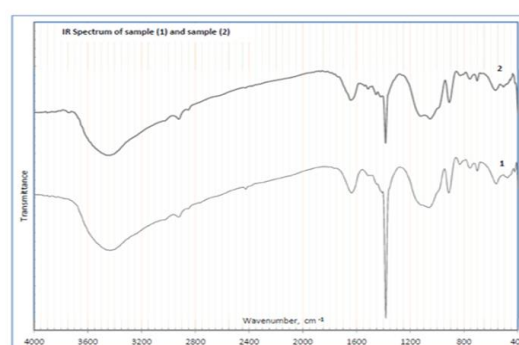


Fig (17): FT-IR spectrum of Purolite C100 (2) before and (1) after uranium adsorption.

3.6. Case study

The uranium removal and recovery from raffinate solutions collected from the solvent extraction unit, Nuclear Materials Authority, Egypt was carried out. For this purpose (5batch) experiments were performed by contacting 0.7 g purolite C100 with 500 mL of the studied liquor for 30 min. By calculating the accumulated loaded uranium, it was found that about 135 mg U/g were adsorbed i.e. 77.1% of the theoretical capacity was realized. The decrease in the C100 capacity after contacting with the raffinate sample may be due to the competition among uranium and different ions in the studied sample, particularly Fe. The chemical composition of the studied mixture before and after treatment is presented in Table (7). The adsorbed uranium has been stripped effectively from loaded purolite C100 using a 1.0 M nitric acid solution. Uranium has been stripped with a stripping efficiency of 94.6%.

Table (7): Chemical composition of the studied raffinate mixture.

Component	Conc., before	Conc., after	Removal, %
Mn	0.108	0.106	2
Fe	0.561	0.481	14.5
Mg	0.198	0.194	2
Ca	0.656	0.636	3
Na	1.238	1.139	8
Al	0.806	0.798	1
K	0.318	0.289	9
U	160 mg/L	25	84

For comparison with the sorption capacity of Purolite C100 with some other sorption capacities for other systems are given in Table (8).

Table (8): The experimental capacity of Purolit C 100 compared with the sorption capacity of other sorbents:

Type	sorption capacity, (mg/ g)	Ref.
Polyethyl eniminephenyl phosphonamidic acid	105.2	[40]
Succinic acid impregnated amberlite XAD-4	65.3	[41]
Gel-amide	81.9	[42]
Natural clinoptilolite zeolite	64	[43]
RHA–aluminum composite	85	[44]
N,N methylene bis-acrylamide (NMBA)	122	[45]
Acrylamide (AAM)	139	[46]
Amberjet 1200 H	133	[47]
Amberlite IR120	106	[15]
Purolit C100	175	Current study

4. Conclusion

The attained results of the present study revealed that Purolite C100 as an adsorbent could be used effectively for uranium removal from the studied nitrate waste aqueous solution (raffinate). Several parameters have been investigated to achieve high sorption efficiency. The preferred sorption conditions were: shaking time of 120 minutes at pH 2.6, room temperature, resin amount is 0.06 gm and agitation speed is 200rpm. Based on these conditions, the resin sorption capacity was about $q_{max} = 175$ mg U/g resin. Kinetic analysis indicated that the sorption results follow the pseudo-second-order-sorption.

Langmuir isotherm model is fitting well with the uranium sorption onto Purolite C100 resin. The value of ' R_L ' indicated favorable sorption of uranium onto Purolite C100. The negative value of ΔH indicates an exothermic nature of uranium adsorption, the positive ΔS parameter suggests increasing the system randomness at the solid-liquid interface during the adsorption process and negative ΔG° indicates that the uranium sorption process is feasible and spontaneous.

References

- [1] C. Zhang, C.J. Dodge, S.V. Malhotra and A.J. Francis, " Bioreduction and precipitation of uranium in ionic liquid aqueous solution by Clostridium sp" Bioresource Tech. 136 (2013), 752-761.
- [2] M.M. Ali, M.H. Taha, H.M. Killa, S. Abd El Wanees and M.M. El-Maadawy " Synergistic extraction of uranium from acidic sulfate leach liquor using D2EHPA mixed with TOPO" J. Radioanal Nucl. Chem. 300 (2014), 963-975.
- [3] M. Solgy, M. Taghizadeh and D. Ghoddocynejad " Adsorption of uranium(VI) from sulphate solutions using Amberlite IRA-402 resin: Equilibrium, kinetics and thermodynamics study" Annals Nucl. Energy. 75 (2015), 132-145.
- [4] C.S. Kedari, S.S. Pandit and P.M. Gandhi, " Separation by competitive transport of uranium(VI) and thorium(IV) nitrates across supported renewable liquid membrane containing trioctylphosphine oxide as metal carrier " J. Membr. Sci. 430 (2013), 188 - 195.
- [5] A. Morsy, M.H. Taha, M. Saeed, A. Waseem, M.A. Riaz and M.M. Elmaadawy " Isothermal, kinetic, and thermodynamic studies for solid-phase extraction of uranium (VI) via hydrazine-impregnated carbon-based material as efficient adsorbent " Nucl. Sci. Techn. 30 (2019), 11 - 23.
- [6] R. Donat, G.K. Cilgi, S. Aytas and H. Cetisl " Thermodynamics Parameters and Sorption of U (VI) on ACSD" Radioanal. and Nucl. Chem. 279 (2009), 271-280.
- [7] International Atomic Energy Agency, Vienna "Uranium Extraction Technology" Technical Reports Series No. 359, 1993.
- [8] R.C. Merritt "The Extractive Metallurgy of Uranium, Colorado School of Mines Research Institute" 1971.
- [9] K. L. Ang, D. Li, N. Aleksandar and N. Nikoloski "The effectiveness of ion exchange resins in separating uranium and thorium from rare earth elements in acidic aqueous sulfate media" Hydrometallurgy. 174(2017), 147-155.
- [10] Y. M. Khawassek, A. M. Masoud, M. H. Taha and A. E. M. Hussein" Kinetics and thermodynamics of uranium ion adsorption from waste solution using Amberjet 1200 H as cation exchanger" J. Radioanal. Nucl. Chem. 315 (2018) ,493–502 .
- [11] Y. M. Khawassek, A. A. Eliwa, E. A. Haggag, S. A. Omar and S. A. Mohamed "Adsorption of rare earth elements by strong acid cation exchange resin thermodynamics, characteristics and kinetics" SN Appl. Sci. 1(2019), 51- 62.
- [12] Y. M. Khawassek, A. A. Eliwa, E. A. Haggag, S. A. Mohamed and S. A. Omar "Equilibrium, Kinetic and Thermodynamics of Uranium Adsorption by Ambersep 400 SO4 Resin" Arab J. Nucl. Sci. Appl. 50(2017), 100-112.
- [13] Z. Wen, K. Huang and Y. Niu " Kinetic study of ultrasonic- assisted uranium adsorption by anion exchange resin" Colloids Surf. 585(2020), 124-131.
- [14] L. Wdkiewicz, R. Dybczyński "Effect of resin cross-linking on the anion-exchange separation of rare earth complexes with DCTA" J Chromatogr. 68(1972),131–141.
- [15] E. A. Gawad "Uranium removal from nitrate solution by cation exchange resin (Amberlite IR 120),

- adsorption and kinetic characteristics" Nucl. Sci. Scien. J. 8(2019), 213- 230.
- [16] M. H. Taha "Solid-liquid extraction of uranium from industrial phosphoric acid using macroporous cation exchange resins: MTC1600H, MTS9500, and MTS9570" Sep. Sci. Tech. 79(2020),199-210
- [17] T.S.Anirudhan, P.G.Radhakrishnan "Kinetics, thermodynamics and surface heterogeneity assessment of uranium(VI) adsorption onto cation exchange resin derived from a lignocellulosic residue" Appl. Surf. Sci. 255(2008), 4983-4991.
- [18] M. M. Abdel Aal and A. A. Abdelsamad "Comparative chemical studies between fixed bed and Batch Dynamic ion exchange techniques for extraction of uranium" Arab J. Nucl. Sci. Applic. 50 (2019), 100-115.
- [19] A. M. Masoud "Sorption behavior of uranium from Sulfate media using purolite A400 as a strong base anion Exchange resin" Inter. J. Env. Anal. Chem. 88(2020), 224-236.
- [20] A. A. Ahmad "Kinetics of uranium adsorption from sulfate medium by a commercial anion exchanger modified with quinoline and silicate", J. Radioanal. Nucl. Chem. 324(2020), 1387-1403.
- [21] S.A. Abo-Farha, A.Y. Abdel-Aal, I. Ashour, S. Garamoun "Removal of some heavy metal cations by synthetic resin purolite C100" J. Hazar. Mat. 169(2009):190-204. 2009
- [22] O. Hamdaoui " Removal of copper(II) from aqueous phase by Purolite C100-MB cation exchange resin in fixed bed columns: modeling" J. Haz. Mat. 161 (2009), 737-746.
- [23] K.J. Mathew, S. Burger, S. Vogt, P. Mason, M.E. Arteaga and U.I. Narayanan " Uranium assay determination using Davies and Gray titration: an overview and implementation of GUM for uncertainty evaluation" J. Radioanal. Nucl. Chem. 282(2009), 939-953.
- [24] Z. Marczenko and M. Balcerzak "Separation, Preconcentration, and Spectrophotometry in Inorganic Analysis" first ed., chapter Principles of Spectrophotometry, p 26-38, Elsevier Science B.V, New York, 2000.
- [25] M. F. Cheira, B. M. Atia, M. N. Kouraim "Uranium(VI) recovery from acidic leach liquor by Ambersep 920U SO₄ resin: kinetic, equilibrium and thermodynamic studies" J. Radiat. Res. Appl. Sci. 10 (2017),307-319.
- [26] M. A. Mahmoud, E. A. Gawad, E.A. Hamoda and E. A. Haggag "Kinetics and Thermodynamic of Fe (III) Adsorption Type onto Activated Carbon from Biomass: Kinetics and Thermodynamics Studies" J. Env. Sci. 11(2015), 128-136.
- [27] S. Lagergren, Handlingar 24 (1898), 1.
- [28] Y.S. Ho and G. McKay " Pseudo-second order model for sorption processes" Proc. Biochem. 34 (1999), 451-465.
- [29] A. A. Abdel-Samad, M. M. Abdel Aal, E. A. Haggag and W. M. Yosef "Synthesis and Characterization of Functionalized activated Carbon for Removal of Uranium and Iron from Phosphoric Acid" J. Bas. Env. Sci. 7 (2020), 140-153.
- [30] E. A. Gawad "A Novel Technique: Conceived Predictive Diagonal (CPD) Graphical Nonlinear Regression Modeling and Simulation" J. Bas. Environ. Sci. 7 (2020), 213-220
- [31] I. Langmuir, Am. Chem. Soc. 40 (9), 1361 (1918).
- [32] H. Freundlich, Phys. Chem. Soc. 40, 1361 (1906).
- [33] S.Dacrory, E.A. Haggag, A.M. Masoud, S.M. Abdo, A.A. Eliwa and S. Kamel "Innovative Synthesis of Modified Cellulose Derivative as a Uranium Adsorbent from Carbonate Solutions of Radioactive Deposits" J. Cellulose. 27 (2020), 7093- 7108.
- [34] M. Manes, L. Hofer and J. Eden "Application of the Polanyi adsorption potential theory to adsorption from solution on activated carbon" J. Phys. Chem. 73(1969), 584-590.
- [35] A. S. El-Sheikh, E. A. Haggag and N. R. Abd El-Rahman" Adsorption of Uranium from Sulfate Medium Using a Synthetic Polymer; Kinetic Characteristics" Radiochem. 62(2020), 499-510.
- [36] K.Y. Foo and B.H. Hameed "Review Insights into the modeling of adsorption isotherm systems" Chem. Eng. J. 156 (2010), 12-22.
- [37] P. Saha and S. Chowdhury "Insight into adsorption thermodynamics" Thermodynamics. 16(2011) ,349-364.
- [38] O. Abderrahim, M. Didi and D. Villemin "A new sorbent for uranium extraction poly ethylenimine phenyl phosphonamidic acid" J. Radioanal. Nucl. Chem. 279(2009), 237-244.
- [39] H.G. Abdien, M.F. Cheira, M.A. Abd-Elraheem, T.A. El-Naser and I.H. Zidan "Extraction and pre-concentration of uranium using activated carbon impregnated trioctyl phosphine oxide" Elix. Inter. J. Appl. Chem. 100 (2016), 43462- 43469.
- [40] A.M. Masoud, W.M. Youssef and A.A. Massoud " Sorption characteristics of uranium from sulfate leach liquor by commercial strong base anion exchange resins" J. Radioanal. Nucl. Chem. 322(2019), 1065-1077.
- [41] Y.M. Khawassek, A.M. Masoud, M.H. Taha and A.E.M. Hussein " Kinetics and thermodynamics of uranium ion adsorption from waste solution using Amberjet 1200 H as cation exchanger" J. Radioanal. Nucl. Chem. 315 (2018), 493 - 502.
- [42] A.A. Younes, A.M. Masoud and M.H. Taha " Uranium sorption from aqueous solutions using polyacrylamide-based chelating sorbents" J. Sep. Sci. Tech. 53 (2018), 2573-2586.
- [43] J. Li, X. Yang, C. Bai, et al. "A novel benzimidazole-functionalized 2-D COF material: synthesis and application as a selective solid-phase extractant for separation of uranium" J. Collo. Interf. Sci. 437(2015), 211- 218.
- [44] E.A. Haggag, A.A. Abdelsamad and A.M. Masoud " Potentiality of uranium extraction from acidic leach liquor by polyacrylamide-acrylic acid titanium silicate composite adsorbent" Inter. J. Environ. Analyt. Chem. 100 (2019), 204 - 224.
- [45] W.M. Youssef, M.S. Hagag and A.H. Ali " Synthesis, characterization and application of composite

derived from rice husk ash with aluminium oxide for sorption of uranium" *Ads. Sci. Tech.* 36(2018), 1274-1293.

[46] F. Semnani, Z. Asadi, M. Samadfam and H. Sepehrian " Uranium(VI) sorption behavior onto amberlite CG-400 anion exchange resin: Effects of pH, contact time, temperature and presence of phosphate" *Ann. Nucl. Ene* 48(2012), 21-24.

[47] M.H. Taha, A.M. Masoud, M.M. El-Maadawy and I.S. ElSayed " Uranium adsorption from Bahariya Oasis leach liquor via TOPO impregnated bentonite material; Isothermal, kinetic and thermodynamic studies" *Egy. J. Chem.* 63(2019), 721 -741.